Original paper

Synoptic Variability of Bio-Optical and Hydrological Parameters off the Crimea Coast According to Data from *in situ* Measurements in Summer 2023

Yu. V. Artamonov, E. A. Skripaleva *, A. A. Latushkin, A. V. Fedirko

Marine Hydrophysical Institute of RAS, Sevastopol, Russia * e-mail: sea-ant@yandex.ru

Abstract

The paper studies the synoptic variability of the light beam attenuation coefficient and intensity of chlorophyll a fluorescence on the sea surface and its relationship with the distributions of hydrological parameters based on the hydrological and bio-optical measurements carried out off the coast of Crimea during the 127th cruise of R/V Professor Vodyanitsky in summer 2023. The measurements were carried out on a finer station grid with the vessel moving from west to east twice with a weekly interval (14-20 June and 22-28 June). It is shown that due to Rim Current penetration into the polygon during the 2nd stage of measurements, the Azov-Kerch waters flew into the polygon water area more intensely. This was accompanied by a decrease in waters transparency and salinity, and an increase in temperature, which was also influenced by the ongoing seasonal heating. In most of the study area, data from both measurement stages revealed a significant tendency of increasing chlorophyll a fluorescence intensity in water areas with a higher beam attenuation coefficient. Changes of the vertical thermohaline and bio-optical waters structure on a scale of about a week were observed in the entire measurement layer and were manifested in changes in the number and values of the maxima of the chlorophyll a fluorescence intensity, the light beam attenuation coefficient, temperature and salinity vertical gradients, as well as their depths. The main maximum of the light beam attenuation coefficient was observed either in the surface layer or in the layer of seasonal thermocline and halocline, while the maximum of the chlorophyll a fluorescence intensity was located under the layer of seasonal thermocline and halocline. The study found a significant linear correlation between the distributions of the depth of the seasonal thermocline and the depths of the maximum of the light beam attenuation coefficient and chlorophyll a fluorescence intensity, as well as between the depths of the seasonal halocline and the maximum intensity of chlorophyll a fluorescence.

Keywords: Black Sea, hydrological stations, light beam attenuation coefficient, chlorophyll a fluorescence, temperature, salinity, water circulation, synoptic variability

Acknowledgements: The work was carried out under FSBSI FRC MHI state assignment FNNN-2024-0014 "Ocean and atmosphere interaction" and FNNN-2024-0012 "Operational Oceanology". The data were obtained at the Center for Collective Use R/V *Professor Vodyanitsky* of FSBSI FRC A.O. Kovalevsky Institute of Biology of the Southern Seas of RAS.

© Artamonov Yu. V., Skripaleva E. A., Latushkin A. A., Fedirko A. V., 2025



This work is licensed under a Creative Commons Attribution-Non Commercial 4.0
International (CC BY-NC 4.0) License

For citation: Artamonov, Yu.V., Skripaleva, E.A., Latushkin, A.A. and Fedirko, A.V., 2025. Synoptic Variability of Bio-Optical and Hydrological Parameters off the Crimea Coast According to Data from *in situ* Measurements in Summer 2023. *Ecological Safety of Coastal and Shelf Zones of Sea*, (3), pp. 6–24.

Синоптическая изменчивость биооптических и гидрологических параметров у берегов Крыма по данным экспедиционных измерений летом 2023 года

Ю. В. Артамонов, Е. А. Скрипалева *, А. А. Латушкин, А. В. Федирко

Морской гидрофизический институт РАН, Севастополь, Россия * e-mail: sea-ant@vandex.ru

Аннотация

По данным гидрологических и биооптических измерений, выполненных у берегов Крыма в ходе 127-го рейса НИС «Профессор Водяницкий» летом 2023 г., исследована синоптическая изменчивость показателя ослабления направленного света и интенсивности флуоресценции хлорофилла a на поверхности моря и ее связь с распределениями гидрологических параметров. Измерения проводили по учащенной сетке станций с продвижением судна с запада на восток дважды с недельным интервалом (14-20 июня и 22-28 июня). Показано, что проникновение потока Основного Черноморского течения на полигон во время 2-го этапа измерений привело к более интенсивному поступлению на акваторию полигона азово-керченских вод. Это сопровождалось понижением прозрачности и солености вод и повышением температуры, на которую также оказывал влияние продолжающийся сезонный прогрев. На большей части полигона, по данным обоих этапов измерений, выявлена значимая тенденция к увеличению интенсивности флуоресценции хлорофилла а в областях вод с повышенными значениями показателя ослабления направленного света. Показано, что изменения вертикальной термохалинной и биооптической структуры вод на масштабе около недели наблюдались во всем слое измерений и проявлялись в изменении количества и значений максимумов интенсивности флуоресценции хлорофилла а, показателя ослабления направленного света, вертикальных градиентов температуры и солености, а также глубин залегания этих параметров. Основной максимум значений показателя ослабления направленного света прослеживался или в поверхностном слое, или в слое сезонных термоклина и галоклина, а максимум интенсивности флуоресценции хлорофилла а располагался под слоем сезонных термоклина и галоклина. Выявлена значимая линейная корреляция между распределениями глубины залегания сезонного термоклина и глубин залегания максимумов показателя ослабления направленного света и интенсивности флуоресценции хлорофилла a, а также между глубинами залегания сезонного галоклина и максимума интенсивности флуоресценции хлорофилла а.

Ключевые слова: Черное море, гидрологические станции, показатель ослабления направленного света, флуоресценция хлорофилла a, температура, соленость, циркуляция вод, синоптическая изменчивость

Благодарности: работа выполнена в рамках тем государственного задания ФГБУН ФИЦ МГИ FNNN-2024-0014 «Взаимодействие океана и атмосферы» и FNNN-2024-0012 «Оперативная океанология». Данные получены в Центре коллективного пользования «НИС Профессор Водяницкий» ФГБУН ФИЦ «Институт биологии южных морей имени А.О. Ковалевского РАН».

Для цитирования: Синоптическая изменчивость биооптических и гидрологических параметров у берегов Крыма по данным экспедиционных измерений летом 2023 года / Ю. В. Артамонов [и др.] // Экологическая безопасность прибрежной и шельфовой зон моря. 2025. № 3. С. 6–24. EDN QEZZHL.

Introduction

In recent years, there has been a noticeable increase in anthropogenic pressure on the coastal part of the Black Sea, making assessments of the ecological state of seawater, which is largely reflected in its hydro-optical structure, increasingly relevant [1, 2]. To assess changes in the ecological state of the waters under the influence of various natural and anthropogenic factors, the light beam attenuation coefficient (LAC) is widely used, which reflects the total suspended solids (TSS) content and characterizes water transparency [3–7]. An important characteristic for assessing primary bioproductivity in water is the content of the photosynthetically active pigment chlorophyll a (*Chl-a*) in marine phytoplankton, determined from measurements of *Chl-a* fluorescence (*F*) or direct measurements [8–13]. In this regard, an important element of environmental monitoring is the study of the variability of LAC and *Chl-a* content at different time scales and the relationship between this variability and the characteristics of the hydrological structure of waters.

Effective monitoring of the hydrological and bio-optical structure of surface waters is conducted using remote sensing methods [2, 14–18]. The use of satellite data has enabled the identification of variability in bio-optical characteristics at different time scales on the surface of the Black Sea [19–22], as well as investigation of the relationship between bio-optical parameters and the thermohaline structure and dynamics of water [23, 24]. According to data from the SeaWiFS and MODIS-Aqua ocean color scanners from the atlas Bio-optical Characteristics of Russian Seas from Satellite Ocean Color Data, Chl-a concentration exhibits two main peaks in the seasonal cycle: spring (March-May) and autumn (October-November). At the same time, the backscattering coefficient of suspended particles exhibits a pronounced maximum in June [20]. Analysis of the climatic seasonal cycle of Chl-a concentration, the diffuse light attenuation coefficient K_d (490), and the remote sensing reflectance R_{rs} (555) based on data from the MODIS-Aqua and NPP-VIIRS satellite scanners from the Copernicus array showed that the main maxima of Chl-a concentration and K_d (490) on the northwestern shelf are observed during the period of the highest water warming rate in May. In the southern part of the western shelf and in the deep-water part of the sea, these maxima occur in November, coinciding with the maximum cooling rate of the water. The maximum R_{rs} (555) values in most of the Black Sea are recorded in June, when the water warms most rapidly [21]. According to data from the MODIS-Aqua

¹⁾ Mankovsky, V.I., Solov'iev, M.V. and Mankovskaya, E.V., 2009. [Hydrooptical Properties of the Black Sea]. A Reference Book. Sevastopol: MGI NAN Ukrainy, 41 p. (in Russian).

ocean color scanner, the influence of the Rim Current (RC) on the distribution of the remote sensing reflectance is observed in April as a band of elevated R_{rs} values above the continental slope [23]. According to Copernicus data, south of the Crimean coast, the influence of the RC on the spatial distribution of average monthly climatic fields of *Chl-a* and R_{rs} (555) is manifested as "tongues" of water with elevated *Chl-a* concentration, R_{rs} (555), temperature, and reduced salinity. The maximum westward spread of waters carried by the RC (almost to 32° E) in the climatic fields of bio-optical and thermohaline parameters is observed in February, during the period of increased zonal geostrophic velocity of the RC [24]. In [22], based on SeaWiFS and MODIS satellite measurements, trends in interannual variability of chlorophyll concentration on the shelf of the northern Black Sea off the Caucasian and Crimean coasts for the period from 1997 to 2015 were analyzed. It was shown that, despite high variability in average annual chlorophyll concentrations across different years, no long-term trend in the distribution of these values was observed, and no pronounced interannual trends were identified [22].

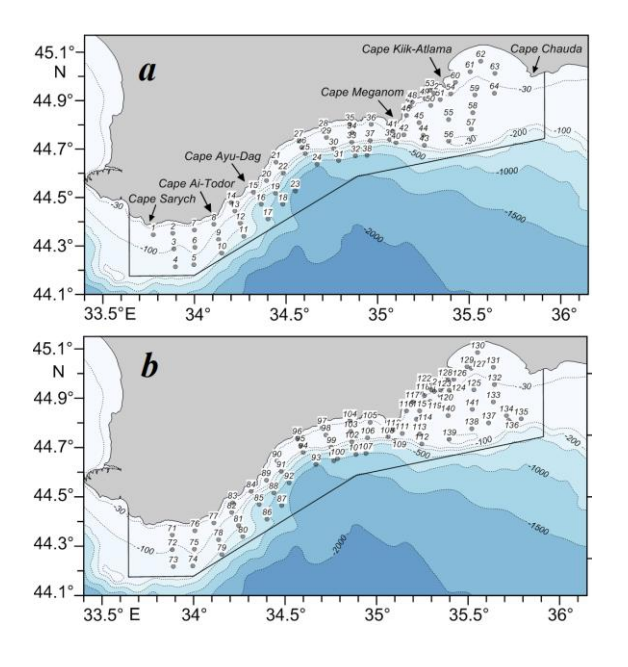
Information about the bio-optical structure of deep-sea waters can only be obtained using contact methods, while conducting hydrological and bio-optical observations quasi-synchronously with instrumental measurements of currents significantly enhances the interpretation of bio-optical field distribution characteristics. Regular expeditionary studies in the northern Black Sea have enabled the assessment of bio-optical and hydrological fields and their variability across various spatial and temporal scales [11, 13, 24-34]. A summary of detailed hydro-optical surveys conducted as part of the expeditionary research program of Marine Hydrophysical Institute of the Russian Academy of Sciences from 2016 to 2020 on R/V Professor Vodyanitsky showed that the main sources of increased TSS concentration in the surface layer off the Crimean coast are low-salinity, turbid waters from the Kerch Strait, riverine inputs from the Caucasian coast, and desalinated waters from the northwestern shelf. In the deep-water part of the sea, localized areas of turbid water were identified, formed under the influence of vertical circulation in regions of cyclonic circulation and meanders of the RC. The vertical structure of TSS concentration was characterized by an upper quasi-homogeneous layer, typically coinciding in thickness with the upper quasi-homogeneous layer of thermohaline parameters. Within this layer, a significant negative linear correlation was observed between TSS concentration and temperature and salinity, while a positive correlation was found with density. In the seasonal thermocline and pycnocline layer, a subsurface maximum of TSS concentration was observed. Below the core of the cold intermediate layer, in the main thermocline, halocline, and pycnocline, an intermediate minimum of TSS concentration was noted. Below this minimum, another layer of increased turbidity was observed, coinciding with the upper boundary of the hydrogen sulfide zone [28].

In June 2023, during the 127th cruise of R/V *Professor Vodyanitsky* in the coastal waters of the Black Sea off the Crimean coast, a comprehensive hydrological and bio-optical survey was conducted, yielding results of particular interest.

Hydrological and bio-optical measurements were performed at a dense network of stations, repeated twice at approximately one-week intervals. The coordinates of the stations surveyed during the two measurement stages were nearly identical, enabling comparison of the measured parameter distributions and assessment of their differences due to synoptic variability. The aim of this study is to analyze the synoptic-scale variability of the light beam attenuation coefficient and *Chl-a* fluorescence distributions off the Crimean coast in the summer of 2023 and to evaluate their relationship with changes in the hydrological structure of the waters.

Materials and methods

Hydrological measurements during the 127th cruise of R/V *Professor Vodyanitsky* in June 2023 were conducted within Russian territorial waters off the Crimean coast, from Cape Sarych to Cape Chauda (Fig. 1). While maintaining the total expedition time (25 days), the measurement area was reduced compared to previous cruises due to administrative restrictions. This allowed for the increased number of hydrological stations, enabling detailed spatial distributions of hydro-optical parameters that reflect the current state of the water structure in the coastal zone of Crimea. The first measurement stage was carried out from June 14 to 20 (64 stations) (Fig. 1, *a*), the second stage from June 22 to 28 (62 stations) (Fig. 1, *b*), with the station coordinates during the two stages almost coinciding.



Seawater temperature (°C) and salinity (PSU) were measured using the IDRONAUT OCEAN SEVEN 320 PlusM CTD probe ²⁾. The speed and direction of currents (cm/s) were measured using a Workhorse Monitor 300 kHz ADCP acoustic Doppler current profiler ³⁾.

Fig. 1. Map of hydrological stations surveyed near Crimean coasts during the 1st (14–20 June 2023) (*a*) and 2nd (22–28 June 2023) (*b*) cruises of R/V *Professor Vodyanitsky*

²⁾ URL: http://www.technopolecom.ru/dounloads/doc_212.pdf

³⁾ URL: https://www.bodc.ac.uk/data/documents/nodb/pdf/workhorse_monitor.pdf

The intensity of chlorophyll a fluorescence (F Chl-a, relative units) and the light beam attenuation coefficient at a wavelength of 660 nm (ϵ_{660} , m⁻¹) were measured using the KONDOR hydrobiophysical multiparametric submersible autonomous complex ⁴, primarily during daylight hours. Additionally, surface wind speed W (m/s) was continuously recorded at each station using the AIRMAR-220WX shipboard weather station.

In quantitative assessments of the consistency of distributions of bio-optical parameters and the depths of their maxima, as well as seasonal thermoclines and haloclines, the statistical reliability of linear correlation coefficients R was evaluated with a statistical significance level of α =0.01 (99% confidence level) according to the methodology ⁵⁾.

Results

During the first measurement stage, the light beam attenuation coefficient varied within the survey area between 0.6 and 0.83 m⁻¹ (Fig. 2, a). The most turbid waters (values $\epsilon_{660} > 0.77$ m⁻¹) were observed in the coastal part of Feodosia Gulf, southeast of Ayu-Dag and at the western boundary of the polygon.

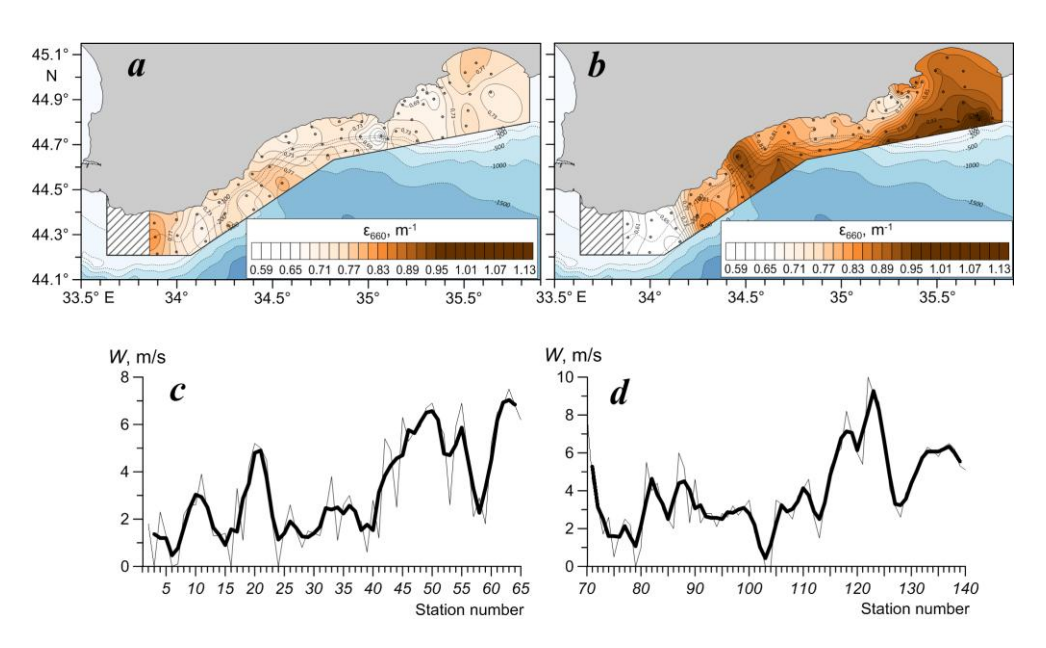


Fig. 2. Distributions of ε_{660} values on the surface (a, b) and wind speed W(c, d) at stations according to data from the 1st (a, c) and 2nd (b, d) stages of the 127th cruise of R/V *Professor Vodyanitsky*. Bold curves in fragments c, d – smoothing by a moving average over three stations

Ecological Safety of Coastal and Shelf Zones of Sea. No. 3. 2025

⁴⁾ Available at: http://ecodevice.com.ru/ecodevice-catalogue/multiturbidimeter-kondor [Accessed: 27 August 2025].

⁵⁾ Malinin, V.N., 2008. [Statistical Methods of Analysis of Hydrometeorological Information]. Saint Petersburg, Izd-vo RGGMU, 408 p. (in Russian).

The increased turbidity in the shallow part of Feodosia Gulf, at depths less than 30 m, was associated with a significant increase in wind speed at stations 61–63 (Fig. 2, c), which caused resuspension of bottom and coastal sediments. The clearest waters (values $\varepsilon_{660} < 0.67 \text{ m}^{-1}$) were observed along the Meganom transect.

During the second stage, one week later, water turbidity at the surface increased significantly across most of the polygon. The ε_{660} values for most of the polygon's water area ranged from 0.65 to 1.15 m⁻¹ (Fig. 2, *b*). The highest ε_{660} values (> 0.91 m⁻¹) were recorded east of Cape Ayu-Dag and at the southern border in the eastern part of the polygon. A noticeable increase in ε_{660} values (0.83–0.89 m⁻¹) was observed near the coast in the area of Cape Kiik-Atlam, where, during the first stage of measurements, ε_{660} values did not exceed 0.73 m⁻¹. As in the coastal part of Feodosia Gulf at stations 61–63, this increase in turbidity was associated with increased wind speed at stations 120–128 (Fig. 2, *d*). The waters with the highest transparency (ε_{660} values < 0.63 m⁻¹) were located at the western border of the polygon, where the highest turbidity was observed during the first stage.

The distribution of F Chl-a intensity on the sea surface during the two measurement stages was highly heterogeneous. For technical reasons, F Chl-a measurements in the first stage began at station 24 (Fig. 3). Consequently, the comparison of F Chl-a distribution was limited to the central and eastern parts of the polygon. During the first measurement stage, F Chl-a values ranged from 0.32 to 0.53 relative units, with a patchy spatial distribution. The highest F Chl-a values (0.47-0.53) relative units) were observed at the southern border of the polygon, approximately between 34.6° and 34.8° E. The lowest F Chl-a values (< 0.35) relative units) were recorded near the coast in the Cape Meganom area and in the eastern part of Feodosia Gulf (Fig. 3, a).

During the second stage of measurements, a general increase in F Chl-a values was observed across almost the entire water area of the polygon (Fig. 3, b). The highest F Chl-a values ranged from 0.59 to 0.61 relative units. The lowest F Chl-a values (< 0.33 relative units), as in the first stage, were observed at the eastern border of the polygon. In the coastal zone near Cape Meganom, where the lowest F Chl-a values were observed during the first stage, a noticeable increase in F Chl-a intensity (0.45–0.50 relative units) was recorded during the second stage (Fig. 3, b).

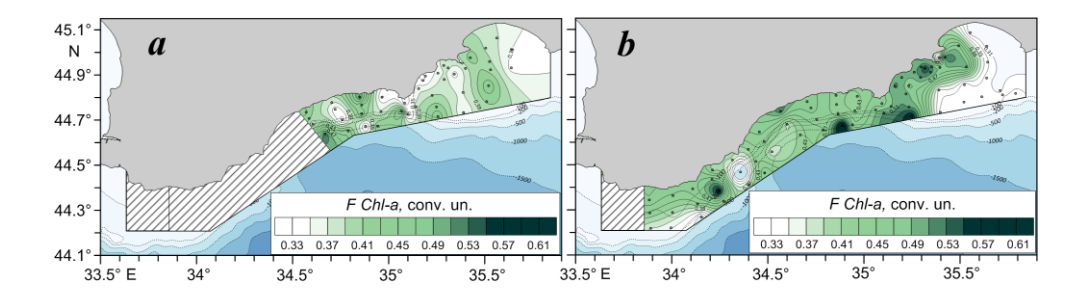


Fig. 3. Distributions of chlorophyll a fluorescence intensity during the $1^{\rm st}$ (a) and $2^{\rm nd}$ (b) stages of the $127^{\rm th}$ cruise of R/V *Professor Vodyanitsky*

Notably, during the second stage, waters at the eastern border of the polygon with reduced F Chl-a intensity were characterized by increased turbidity (Fig. 2, b; 3, b).

Overall, despite the observed differences in the distribution of the light beam attenuation coefficient and F *Chl-a* intensity between the first and second stages, a significant trend of increasing F *Chl-a* intensity was identified in areas of elevated water turbidity across most of the polygon (Fig. 4). The exception is the water area at the eastern border of the polygon, characterized by increased turbidity during the second stage. In this area, a decrease in F *Chl-a* intensity was observed (Fig. 2, b; 3, b; 4, c).

Analysis of the distribution of flow vectors based on instrumental measurements showed that differences between the distribution of ϵ_{660} values during the two measurement stages were associated with noticeable changes in water circulation (Fig. 5). Thus, the main westward flow characterizing the RC was most clearly traced only in the western part of the polygon during the first stage, while east of Cape Ai-Todor, a flow in the opposite eastern direction was observed (Fig. 5, a). In the eastern part of the polygon, well-defined synoptic vortices were observed – cyclonic south of Feodosia Gulf (Feodosia cyclone) and anticyclonic slightly west of the Karadag traverse (Karadag anticyclone). This water circulation pattern shows that over most of the water area east of Cape Ai-Todor, the main RC flow was located further south, outside the polygon.

During the second stage, the circulation pattern changed significantly (Fig. 5, b). Across most of the water area, except for Feodosia Gulf, westward currents corresponding to the RC flow were observed. In the central part of the polygon, one branch of the RC flow turned north, then northeast, forming the Crimean anticyclone, while the other branch continued westward.

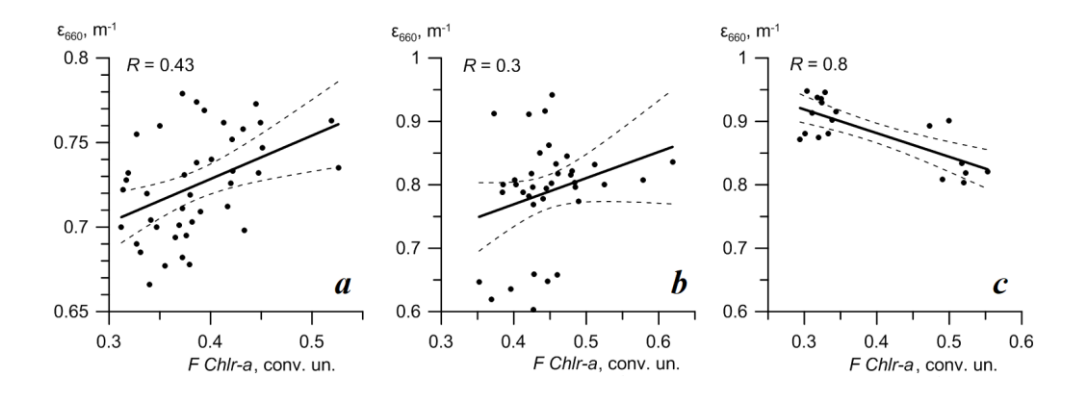


Fig. 4. Graphs of the linear correlation between the values of F Chl-a and ϵ_{660} according to the data of the 1st stage at stations 24–65 (a), the 2nd stage at stations 71–119 (b) and 120–141 (c). Dashed lines are the boundaries of the 99% confidence interval

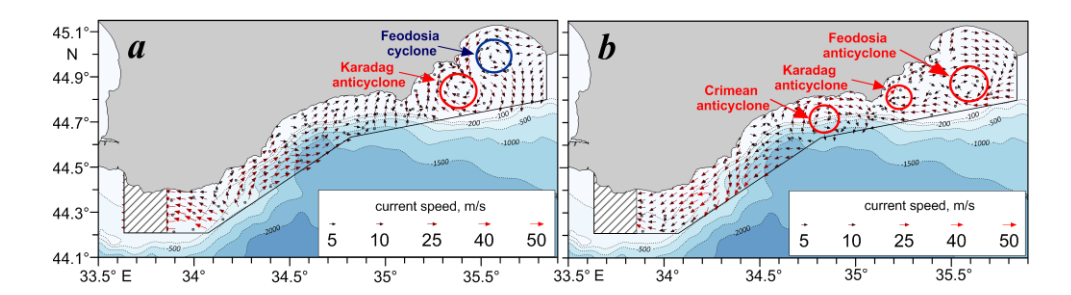


Fig. 5. Distributions of vectors of instrumentally measured currents (cm/s) in the surface layer according to data from the 1^{st} (a) and 2^{nd} (b) stages of the 127^{th} cruise of R/V *Professor Vodyanitsky*. Anticyclonic eddies are shown in red, cyclonic eddies are shown in blue

The Karadag anticyclone persisted in the eastern part of the polygon. Instead of the Feodosia cyclone, an anticyclonic vortex formed closer to the southern border of the polygon, provisionally named the Feodosia anticyclone (Fig. 5, b).

The distributions of temperature (TPM) and salinity (SPM) at the sea surface during the two measurement stages differed significantly (Fig. 6). Weekly temporal changes were evident in a noticeable increase in TPM values (22.6–25.3°C) during the second stage compared to the first stage, when TPM values ranged from 20.6 to 23.4°C (Fig. 6, a, b). This increase in TPM was associated with both ongoing seasonal warming of surface waters, as the second stage occurred one week later, and the inflow of water into the polygon's water area, carried by the RC flow from the southeast to the shores of Crimea. These waters were characterized by elevated temperatures and reduced salinity [24], which was associated with the influence of the Azov-Kerch desalination, in which Azov Sea waters penetrate through the Kerch Strait and move westward along the northern periphery of the RC [24, 35]. The influence of Azov-Kerch desalination on the salinity field at the sea surface (Fig. 6, c, d) was most clearly evident during the second stage of measurements in the central part of the polygon. Desalinated waters with SPM values below 17.9 PSU, carried by the RC flow, spread along the periphery of the Crimean anticyclone to the northeast, then followed the coast in an easterly direction and further to the southeast (Fig. 6, d).

In addition to reduced salinity, the Azov-Kerch waters are also characterized by increased turbidity [24, 35], which led to an increase in ε_{660} values during the second stage of measurements, most evident in the southeastern and central parts of

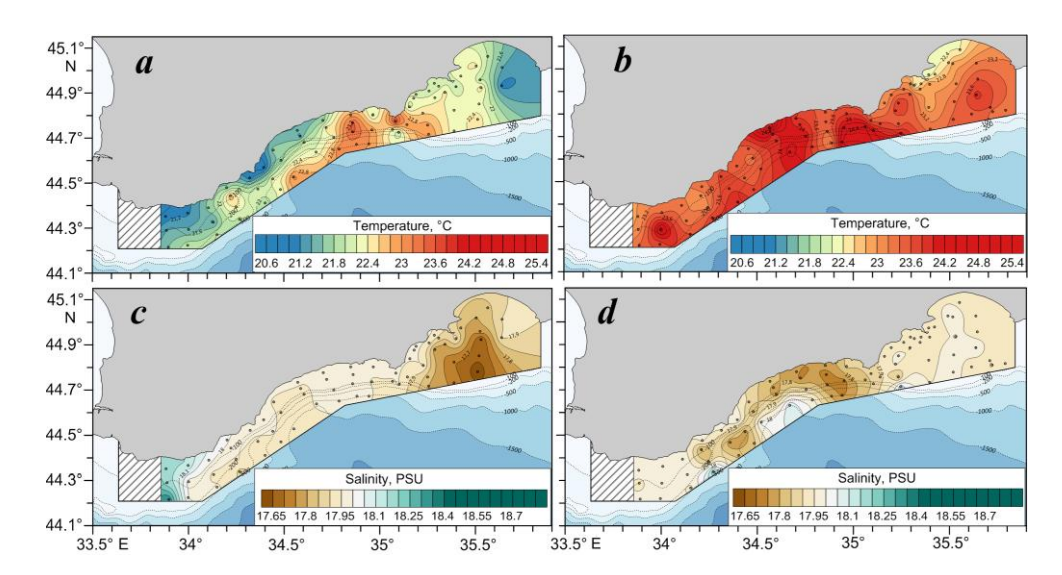


Fig. 6. Distributions of temperature (a, b) and salinity (c, d) at the 2 m horizon according to data from the 1st (a, c) and 2nd (b, d) stages of the 127th cruise of R/V *Professor Vodyanitsky*

the polygon (Fig. 2, b). Notably, in the eastern part of the polygon, where increased turbidity was observed during the second stage, a noticeable decrease in *Chl-a* fluorescence intensity was recorded. This may be associated with the penetration of Azov-Kerch waters into the southeastern part of the polygon, which then spread along the periphery of the Feodosia anticyclone to the entire eastern part of the water area. According to [36], during the measurement period (June), the concentration of *Chl-a* in the Sea of Azov reaches its lowest values.

Thus, changes in the distribution of the light beam attenuation coefficient, temperature, and salinity at the sea surface on a synoptic time scale (approximately one week) were primarily due to variability in water circulation. The penetration of the RC flow into the polygon during the second stage of measurements led to a more intensive inflow of Azov-Kerch waters into the polygon's water area, which was accompanied by a decrease in transparency and salinity and an increase in temperature, further influenced by ongoing seasonal warming.

The vertical distribution of the light beam attenuation coefficient, F Chl-a intensity, temperature, and salinity showed that the thermohaline and biooptical fields were characterized by well-defined summer vertical stratification. Examples of vertical profiles of ε_{660} , F Chl-a, and vertical gradients of temperature (VTG) and salinity (VSG) at stations measured at the same point at weekly intervals in different parts of the polygon are shown in Fig. 7. Synoptic changes in the vertical bio-optical and thermohaline structure of the water column on a scale of approximately one week were observed throughout the measurement layer and were evident in changes in the number and magnitude of the ε_{660} , F Chl-a, VTG (in absolute terms) and VSG maxima, as well as their depths.

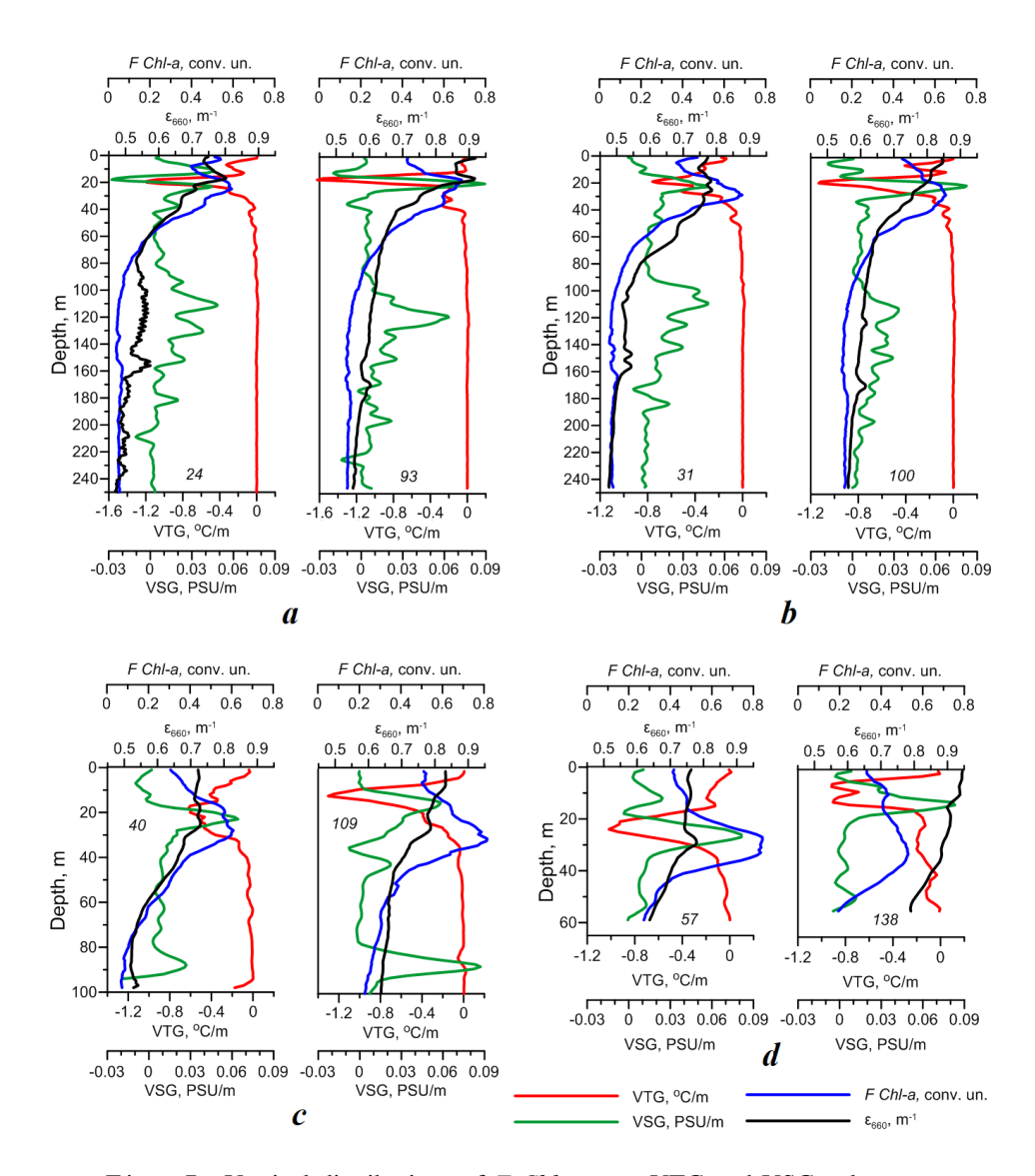


Fig. 7. Vertical distributions of F Chl-a, ϵ_{660} , VTG and VSG values at stations carried out at the same point with a weekly interval in different parts of the polygon. The station numbers are indicated on the graphs

For example, at station 24 (stage 1), one main ε_{660} maximum (0.8 m⁻¹) was observed at a depth of 18 m. One week later (station 93, stage 2), two ε_{660} maxima (0.92 m⁻¹) were observed – at the surface and at a depth of 16 m. The main *F Chl-a* intensity maximum at station 24 was located at a depth of 25 m, while at station 93, it was at a depth of 18 m, with its value increasing from 0.6 to 0.7 relative units (Fig. 7, *a*).

The thermohaline structure at station 24 was characterized by one main maximum VTG (1.2°C/m) at a depth of 20 m and two maximum VSG (0.045 PSU/m) at depths of 11 m and 22 m. One week later (station 93), one maximum VTG and VSG were observed at depths of 18–20 m, with values increasing to 1.6°C/m and 0.09 PSU/m, respectively (Fig. 7, a).

Further east, at station 31 (stage 1), two maxima of ε_{660} (0.78 m⁻¹) were detected at depths of 18 m and 23 m. One week later (station 100), ε_{660} maxima (0.85 m⁻¹) were observed in the surface layer. The maximum F *Chl-a* intensity, based on data from both stages, was located at a depth of 30 m, with its value decreasing from 0.7 relative units (station 31) to 0.65 relative units (station 100) (Fig. 7, b). The seasonal thermocline (VTG ~ 0.78 °C/m) and halocline (VSG ~ 0.05 PSU/m) at station 31 were located at depths of 20–21 m. One week later (station 100), their depth remained unchanged, but their values increased to 1.17°C/m and 0.08 PSU/m, respectively (Fig. 7, b).

In the Cape Meganom area at station 40 (stage 1), maxima of ϵ_{660} (0.74 m⁻¹) were observed at depths of 18 m and 25 m. One week later (station 109), these maxima increased to 0.84 m⁻¹ and were observed in the surface layer at depths of 2–7 m. The maximum F *Chl-a* intensity at stations 40 and 109 was detected at depths of 28 m and 32 m, respectively, with its value increasing from 0.6 to 0.8 relative units (Fig. 7, c). The maximum VTG value increased from 0.6°C/m (station 40) to 1.3°C/m (station 109). The maximum VSG values at both stations ranged from 0.06 to 0.063 PSU/m. The depths of the seasonal thermocline and halocline decreased from 18 m and 22 m at station 40 to 12 m and 15 m at station 109 (Fig. 7, c).

In the eastern part of the polygon, at shallow station 57, the main maxima ϵ_{660} (0.77 m⁻¹) were observed at a depth of 30 m. One week later (station 138), the ϵ_{660} maxima (0.95 m⁻¹) were observed in the surface layer at depths of 2–10 m. The maximum F *Chl-a* intensity, in contrast, decreased from 0.95 relative units (station 57) to 0.77 relative units (station 138). It was observed in the layer 27–32 m at station 57 and at a depth of 32 m at station 138 (Fig. 7, d). The depths of the VTG and VSG maxima at station 57 were 24 m and 27 m, respectively. At station 138, two well-defined VTG maxima were observed at depths of 5 m and 12 m, while the depth of the VSG maximum decreased to 12 m. The maximum VTG values decreased from 1°C/m (station 57) to 0.9°C/m (station 138), and the maximum VSG values at both stations ranged from 0.080 to 0.082 PSU/m (Fig. 7, d).

Notably, at deep-water stations, another maximum of ε_{660} was observed below the main halocline, located approximately in the 150–170 m layer (Fig. 7, a, b), which, according to [37], corresponds to the lower boundary of the suboxic redox zone and the upper layer of the hydrogen sulfide zone. According to previous expedition measurements, a maximum concentration of TSS was also detected at these depths [29, 30]. This increase in ε_{660} values (up to 0.6 m⁻¹) was observed in both measurement stages, but the depth of these maxima varied by 10–15 m over the week (Fig. 7, a, b).

Overall, during the second stage of measurements, an increase in the maximum VTG (Fig. 8, a) and VSG (Fig. 8, b) values was observed across most of the polygon, indicating more pronounced vertical thermohaline stratification. In the subsurface layer, there was also an increase in ϵ_{660} values, particularly in the eastern part of the polygon (Fig. 8, c), an increase in F Chl-a intensity across most of the polygon, and a decrease in these values in the eastern part of the polygon (Fig. 8, d).

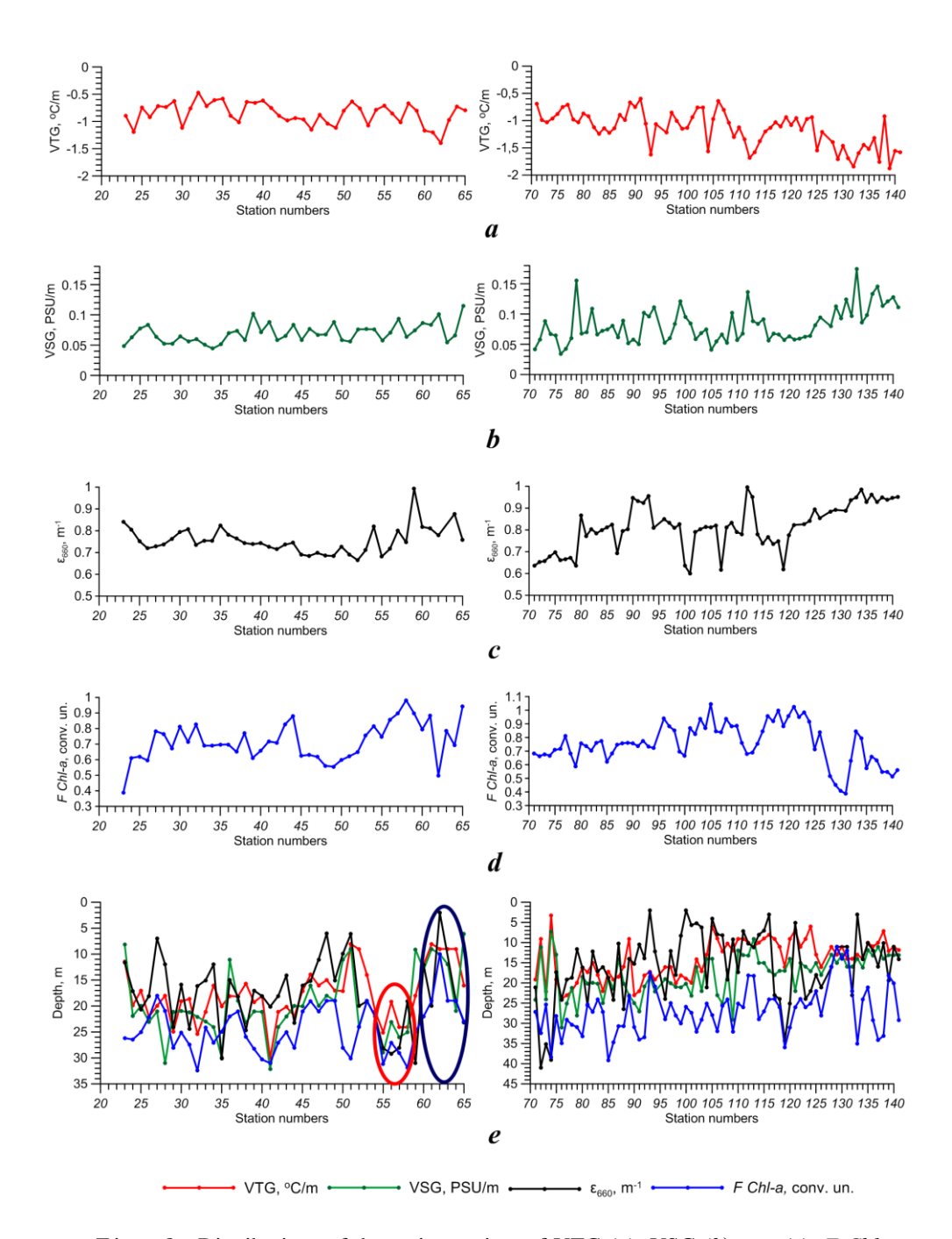


Fig. 8. Distributions of the main maxima of VTG (a), VSG (b), ε_{660} (c), F Chl-a (d) values, their depths (e) at stations according to data from the 1st (left) and 2nd (right) stages of the 127th cruise of R/V Professor Vodyanitsky. The red ellipse highlights the depths of the parameters at stations located in the area of the Karadag anticyclone, and the blue ellipse highlights the depths of the parameters at stations located in the area of the Feodosia cyclone.

The distribution of the depths of the main maxima of VTG, VSG, ε_{660} and F Chl-a intensity at all stations showed that the depths of the seasonal thermocline during the first stage ranged from 7 to 30 m, while during the second stage, the thermocline rose closer to the surface and was located at depths of 4–24 m (Fig. 8, e). The seasonal halocline was observed at depths of 6 to 32 m during both stages (Fig. 8, e). Analysis of vertical profiles of ε_{660} values during both stages showed that the maximum ε_{660} values were observed either in the surface layer or within the seasonal thermocline and halocline layers, consistent with the depth of the maximum concentration of TSS according to long-term expedition measurements [28]. According to data from all stations, the maximum F Chl-a intensity was located below the seasonal thermocline and halocline layers (Fig. 8, e). The distribution of depths of the maximum thermohaline and bio-optical parameters during the first stage of measurements clearly showed the dynamics of water masses. There was a noticeable increase in these depths at stations located in the Karadag anticyclone area (stations 54–59, highlighted with a red ellipse) and a decrease at stations in the Feodosia cyclone area (stations 60–65, highlighted with a blue ellipse) (Fig. 8, e). Analysis of the vertical structure of water circulation showed that these synoptic vortices were clearly visible throughout the entire upper 50 m layer.

During the second stage of measurements, synoptic anticyclonic vortices were evident only in the upper 10 m layer, so the circulation features were minimally reflected in the distribution of the depths of the thermohaline and bio-optical parameters (Fig. 8, *e*).

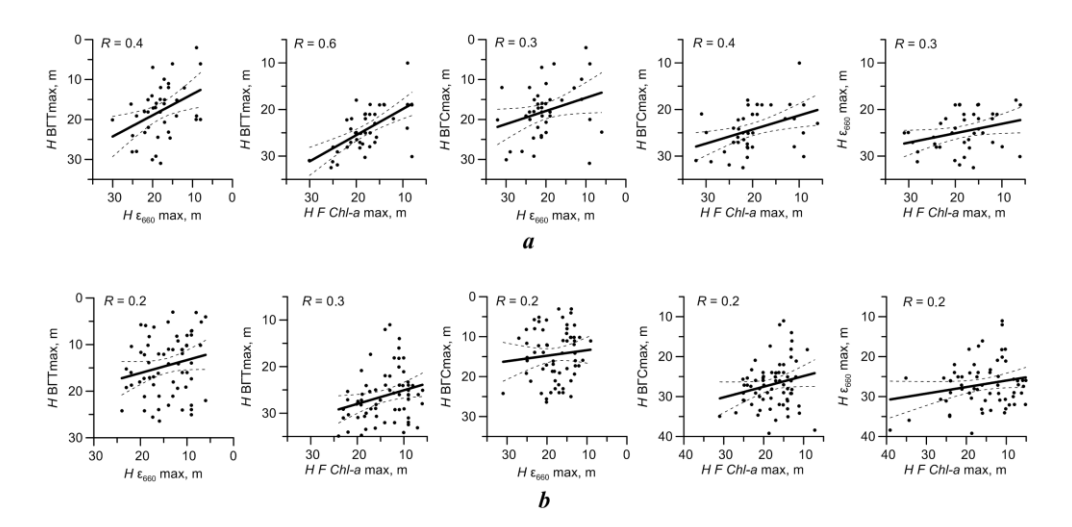


Fig. 9. Graphs of the linear correlation between the depths of occurrence of the maxima of F *Chl-a*, ε_{660} , VTG and VSG according to the data of the 1^{st} (a) and 2^{nd} (b) stages of the 127^{th} cruise of R/V *Professor Vodyanitsky*. Dashed lines are the boundaries of the confidence interval of the 99% level of statistical significance

Quantitative assessments of the consistency of the distributions of the depths of the maximum bio-optical parameters and the seasonal thermocline and halocline (Fig. 9) showed that the strongest relationship between these parameters was observed during the first stage of measurements (Fig. 9, a). A significant direct linear correlation, with a statistical significance level of $\alpha = 0.01$ (99% confidence level), was found between the depth of the seasonal thermocline and the depths of the maximum ε_{660} and F Chl-a intensity, as well as between the depths of the seasonal halocline and the maximum F Chl-a intensity. The correlation coefficients R for these relationships were 0.4, 0.6, and 0.4, respectively. The linear correlation between the depth of the seasonal halocline and the maximum ε_{660} , as well as between the maxima of ε_{660} and F Chl-a, was weaker, with R values of 0.3 (Fig. 9, a).

During the second stage of measurements, the relationship between the distributions of the depths of the maximum bio-optical parameters and the seasonal thermocline and halocline remained significant at $\alpha = 0.01$, but weakened noticeably, with *R* values not exceeding 0.3 (Fig. 9, *b*).

Conclusions

According to hydrological and bio-optical measurements conducted in June 2023 during the 127th cruise of R/V Professor Vodyanitsky off the coast of Crimea, the variability of the distribution of the light beam attenuation coefficient and F Chl-a intensity on a synoptic scale was analyzed, and the relationship between this variability and changes in the hydrological structure of the waters was assessed. Across most of the polygon, data from both measurement stages revealed a significant trend of increasing F Chl-a intensity in areas with elevated light beam attenuation coefficient values. It was shown that changes in the distribution of temperature, salinity, and LAC values at the sea surface on a weekly time scale were associated with changes in water circulation. During the second stage of measurements, warmer, less saline, and more turbid Azov-Kerch waters penetrated the polygon with the RC flow, leading to a decrease in salinity in the central part of the polygon, an increase in turbidity in the southeastern and central parts of the polygon, and an increase in temperature, further influenced by ongoing seasonal warming. The Azov-Kerch waters entering the southeastern part of the polygon and then spreading to the entire eastern part of the water area along the periphery of the Feodosia anticyclone contributed to a decrease in F Chl-a intensity in the area of increased turbidity at the eastern border of the polygon, as the concentration of *Chl-a* in the Sea of Azov during the measurement period was reduced.

It has been shown that synoptic changes in the vertical thermohaline and biooptical structure of waters on a scale of approximately one week were observed throughout the measurement layer and were evident in changes in the number and magnitude of the maxima of LAC, *F Chl-a*, VTG and VSG, as well as their depths. During the second stage of measurements, thermohaline fields were characterized by more pronounced vertical stratification across most of the polygon. In the subsurface layer, as at the surface, there was an increase in LAC values, particularly in the eastern part of the polygon, an increase in *F Chl-a* intensity across most of the polygon, and a decrease in these values in the eastern part of the polygon. The main LAC maxima were observed either in the surface layer or within the seasonal thermocline and halocline layers, while the maximum *F Chl-a* intensity was located below the seasonal thermocline and halocline layers. At deep-water stations, another LAC maximum was observed below the main halocline layer, located in the 150–170 m layer, corresponding to the lower boundary of the suboxic redox zone and the upper layer of the hydrogen sulfide zone.

A significant linear correlation was found between the depth of the seasonal thermocline and the depths of the maximum LAC values and F Chl-a intensity, as well as between the depth of the seasonal halocline and the maximum F Chl-a intensity, based on data from the first stage of measurements, with R coefficients of 0.4, 0.6, and 0.4, respectively.

REFERENCES

- 1. Ivanov, V.A., Katunina, E.V. and Sovga, E.E., 2016. Assessment of Anthropogenic Impacts on the Ecosystem of the Waters of the Herakleian Peninsula in the Vicinity of Deep Drains, *Processes in GeoMedia*, (5), pp. 62–68 (in Russian).
- Bondur, V.G., Ivanov, V.A., Vorobiev, V.E., Dulov, V.A., Dolotov, V.V., Zamshin, V.V., Kondratiev, S.I., Lee, M.E. and Malinovsky, V.V., 2020. Ground-to-Space Monitoring of Anthropogenic Impacts on the Coastal Zone of the Crimean Peninsula. *Physical Oceanography*, 27(1), pp. 95-107. https://doi.org/10.22449/1573-160X-2020-1-95-107
- 3. Eisma, D., 1993. *Suspended Matter in the Aquatic Environment*. Berlin, Heidelberg: Springer-Verlag, 315 p. https://doi.org/10.1007/978-3-642-77722-6
- 4. Man'kovskii, V.I. and Solov'ev, M.V., 2003 Relationship between the Beam Attenuation Coefficient and the Concentration of Suspended Matter in Black-Sea Waters. *Physical Oceanography*, 13(2), 123–128. https://doi.org/10.1023/A:1023752514790
- 5. Izrael, Yu.A. and Tsyban, A.V., 2009. [Anthropogenic Ecology of the Ocean]. Moscow: Flinta, 520 p. (in Russian).
- 6. Kukushkin, A.S., Agafonov, E.A. and Prokhorenko, Yu.A., 2006. Distribution of the Beam Attenuation Coefficient in the Black Sea Surface Coastal Waters. *Morskoy Gidrofizicheskiy Zhurnal*, (5), pp. 30–43 (in Russian).
- 7. Kukushkin, A.S., 2017. Spatial and Temporal Variability of the Water Transparency Distribution in the North-Western Black Sea. *Atmospheric and Oceanic Optics*, 30(9), pp. 750–762. https://doi.org/10.15372/AOO20170904 (in Russian).
- 8. Hoepffner, N. and Sathyendranath, S., 1992 Bio-Optical Characteristics of Coastal Waters: Absorption Spectra of Phytoplankton and Pigment Distribution in the Western North Atlantic. *Limnology and Oceanography*, 37(8), pp. 1660–1679. https://doi.org/10.4319/lo.1992.37.8.1660
- 9. McManus, G.B. and Dawson, R., 1994. Phytoplankton Pigments in the Deep Chlorophyll Maximum of the Caribbean Sea and the Western Tropical Atlantic Ocean. *Marine Ecology Progress Series*, 113, pp. 199–206. https://doi.org/10.3354/meps113199
- 10. Mordasova, N.V., 2014. Indirect Estimation of Water Productivity by the Chlorophyll Content. *Trudy VNIRO*, 152, pp. 41–56 (in Russian).

- Moiseeva, N.A., Churilova, T.Ya., Efimova, T.V., Krivenko, O.V. and Matorin, D.N., 2019. Fluorescence of Chlorophyll a During Seasonal Water Stratification in the Black Sea. *Physical Oceanography*, 26(5), pp. 425–437. https://doi.org/10.22449/1573-160X-2019-5-425-437
- 12. Temerdashev, Z.A., Pavlenko, L.F., Ermakova, Ya.S., Korpakova, I.G. and Eletskii, B.D., 2019. Extraction-Fluorimetric Determination of Chlorophyll "A" in the Natural Waters. *Analytics and Control*, 23(3), pp. 323–333 (in Russian).
- 13. Mansurova, I.M., Stelmakh, L.V. and Farber, A.A., 2023. Vertical Distribution of Chlorophyll "A" Concentration in the Black Sea in the Summer and Autumn Periods according to the Data of the Probe CTD Complex and Direct Measurements. *Monitoring systems of environment*, (2), pp. 84–91 (in Russian).
- 14. Volpe, V., Silvestri, S. and Marani, M., 2011. Remote sensing retrieval of suspended sediment concentration in shallow waters. *Remote Sensing of Environment*, 115(1), pp. 44–54. https://doi.org/10.1016/j.rse.2010.07.013
- 15. Kremenchutskiy, D.A., Kubryakov, A.A., Zav'yalov, P.O., Konovalov, B.V., Stanichniy, S.V. and Aleskerova, A.A., 2014. Determination of the Suspended Matter Concentration in the Black Sea Using to the Satellite MODIS Data. In: MHI, 2014. *Ekologicheskaya Bezopasnost' Pribrezhnoy i Shel'fovoy Zon i Kompleksnoe Ispol'zovanie Resursov Shel'fa* [Ecological Safety of Coastal and Shelf Zones and Comprehensive Use of Shelf Resources]. Sevastopol: ECOSI-Gidrofizika. Iss. 29, pp. 5–9 (in Russian).
- 16. Suslin, V.V., Churilova, T.Ya., Lee, M., Moncheva, S. and Finenko, Z.Z., 2018. Comparison of the Black Sea Chlorophyll-A Algorithms for SeaWIFS and Modis Instruments. *Fundamental and Applied Hydrophysics*, 11(3), pp. 64–72. https://doi.org/10.7868/S2073667318030085 (in Russian).
- 17. Xiaolong, Y., Zhongping, L., Fang, S., Menghua, W., Jianwei, W., Lide, J. and Zhehai, S., 2019. An Empirical Algorithm to Seamlessly Retrieve the Concentration of Suspended Particulate Matter from Water Color across Ocean to Turbid River Mouths. *Remote Sensing of Environment*, 235, 111491. https://doi.org/10.1016/j.rse.2019.111491
- Zamshin, V.V., Matrosova, E.R., Khodaeva, V.N. and Chvertkova, O.I., 2021.
 Quantitative Approach to Studying Film Pollution of the Sea Surface Using Satellite Imagery. *Physical Oceanography*, 28(5), pp. 567–578. https://doi.org/10.22449/1573-160X-2021-5-567-578
- 19. Suetin, V.S., Suslin, V.V., Korolev, S.N. and Kucheryavyi, A.A., 2002. Analysis of the Variability of the Optical Properties of Water in the Black Sea in Summer 1998 according to the Data of a SeaWiFS Satellite Instrument. *Physical Oceanography*, 12(6), pp. 331–340. https://doi.org/10.1023/A:1021729229168
- Kopelevich, O.V., Sheberstov, S.V., Saling, I.V., Vazyulya, S.V. and Burenkov, V.I., 2015. Seasonal and Inter-Annual Changeability of Bio-Optical Characteristics in the Surface Layer of the Barents, White, Black and Caspian Seas from Satellite Data. *Fundamental and Applied Hydrophysics*, 8(1), pp. 7–16 (in Russian).
- 21. Artamonov, Yu.V., Skripaleva, E.A., Latushkin, A.A. and Fedirko, A.V., 2019. Multi-Year Average Intra-Annual Cycle of Hydrooptical Characteristics, Chlorophyll A and Surface Temperature of the Black Sea from Satellite Data. *Sovremennye Problemy Distantsionnogo Zondirovaniya Zemli iz Kosmosa*, 16(1), pp. 171–180 (in Russian).
- Kovalyova, I.V., Finenko, Z.Z. and Suslin, V.V., 2021. Trends of Long-Term Changes in Chlorophyll Concentration, Primary Production of Phytoplankton and Water Temperature in the Shelf Regions of the Black Sea. Sovremennye Problemy Distantsionnogo Zondirovaniya Zemli iz Kosmosa, 18(4), pp. 228–235 (in Russian).

- 23. Karabashev, G.S. and Evdoshenko, M.A., 2015. Manifestations of the Rim Current, Coccolithophore Blooms, And Continental Runoff in the Long-Term Monthly Mean Distributions of Satellite Reflectance Coefficients of the Black Sea. *Oceanology*, 55(1), pp. 36–46. https://doi.org/10.1134/S0001437015010087
- 24. Artamonov, Yu.V., Latushkin, A.A., Skripaleva, E.A. and Fedirko, A.V., 2019. Rim Current Manifestation in the Climatic Fields of Hydro-Optical and Hydrological Characteristics at the Coast of Crimea. In: SPIE, 2019. *Proceedings of SPIE*. Bellingham: SPIE. Vol. 11208: 25th International Symposium on Atmospheric and Ocean Optics: Atmospheric Physics, 112084X. https://doi.org/10.1117/12.2540803
- 25. Lomakin, P.D., Chepyzhenko, A.I. and Chepyzhenko, A.A., 2007. Estimation to concentrations of total suspension and dissolved organic matter of the artificial origin in the bays of the Crimea according to optical measurements. In: MHI, 2007. Ekologicheskaya Bezopasnost' Pribrezhnoy i Shel'fovoy Zon i Kompleksnoe Ispol'zovanie Resursov Shel'fa [Ecological Safety of Coastal and Shelf Zones and Comprehensive Use of Shelf Resources]. Sevastopol: MHI. Iss. 15, pp. 168–176 (in Russian).
- 26. Lee, M.E., Latushkin, A.A. and Martynov, O.V., 2018. Long-Term Transparency Variability of the Black Sea Surface Waters. *Fundamental and Applied Hydrophysics*, 11(3), pp. 40–46. https://doi.org/10.7868/S207366731803005X (in Russian).
- Efimova, T.V., Churilova, T.Ya., Skorokhod, E.Yu., Moiseeva, N.A. and Zemlianskaia, E.A., 2020. Vertical Distribution of Bio-Optical Properties of the Azov Black Sea Basin Waters in April May, 2019. *Physical Oceanography*, 27(5), pp. 525–534. https://doi.org/10.22449/1573-160X-2020-5-525-534
- 28. Latushkin, A.A., Artamonov, Yu.V., Skripaleva, E.A. and Fedirko, A.V., 2022. The Relationship of the Spatial Structure of the Total Suspended Matter Concentration and Hydrological Parameters in the Northern Black Sea according to Contact Measurements. *Fundamental and Applied Hydrophysics*, 15(2), pp. 124–137. https://doi.org/10.48612/fpg/4heu-kxbn-gg7t (in Russian).
- 29. Artamonov, Yu.V., Skripaleva, E.A., Latushkin, A.A., Fedirko, A.V. and Ryabokon, D.A., 2022. Hydrological Water Structure and Distribution of Total Suspended Matter off the Coast of Crimea in Spring 2021. *Ecological Safety of Coastal and Shelf Zones of Sea*, (4), pp. 6–24.
- 30. Stelmakh, L., Kovrigina, N. and Gorbunova, T., 2023. Phytoplankton Seasonal Dynamics under Conditions of Climate Change and Anthropogenic Pollution in the Western Coastal Waters of the Black Sea (Sevastopol Region). *Journal of Marine Science and Engineering*, 11(3), 569. https://doi.org/10.3390/jmse11030569
- 31. Latushkin, A.A., Artamonov, Yu.V., Skripaleva, E.A. and Fedirko, A.V., 2023. Spatial Structure of Turbidity and Chlorophyl-A Fields near the Crimean Coasts according to Natural Measurement In July 2022. In: IO RAS, 2023. Proceedings of the XII All-Russian Conference with International Participation "Current Problems in Optics of Natural Waters". 25–27 October 2023, Saint Petersburg. Vol. 13. Moscow: Shirshov Institute Publishing House, pp. 92–96 (in Russian).
- 32. Krasheninnikova, S.B. and Babich, S.A., 2022. Spatial Distribution of Chlorophyll-A Concentration in Hydrological, Hydrochemical and Hydroptical Conditions of the Black Sea in Spring 2021. *Proceedings of the T.I.Vyazemsky Karadag Scientific Station Nature Reserve of the Russian Academy of Sciences*. (3), pp. 13–22 (in Russian).
- 33. Korchemkina, E.N. and Mankovskaya, E.V., 2024. Spectral Reflectance Coefficient, Color Characteristics and Relative Transparency of the Black Sea Waters in Spring, 2019 and 2021: Comparative Variability and Empirical Relationships. *Physical Oceanography*, 31(1), pp. 3–17.

- 34. Piontkovski, S.A., Zagorodnyaya, Yu.A., Serikova, I.M., Minski, I.A., Kovaleva, I.V. and Georgieva, E.Yu., 2024. Interannual Variability of Physical and Biological Characteristics of Crimean Shelf Waters in Summer Season (2010–2020). *Ecological Safety of Coastal and Shelf Zones of Sea*, (2), pp. 39–59.
- 35. Aleskerova, A.A., Kubryakov, A.A., Goryachkin, Yu.N. and Stanichny, S.V., 2017. Propagation of Waters from the Kerch Strait in the Black Sea. *Physical Oceanography*, (6), pp. 47–57. https://doi.org/10.22449/1573-160X-2017-6-47-57
- 36. Saprygin, V.V., Berdnikov, S.V., Kulygin, V.V., Dashkevich, L.V. and Mestetskiy, L.M., 2018. Spatial Distribution and Seasonal Dynamics of the Chlorophyll A Concentration in the Sea of Azov Based on MERIS Images. *Oceanology*, 58(5), pp. 689–699. https://doi.org/10.1134/S0001437018050132
- Yakushev, E.V., Chasovnikov, V.K., Podymov, O.I., Pakhomova, S.V., Stunzhas, P.A. and Murray, J.W., 2008. Vertical Hydro-Chemical Structure of the Black Sea. In: A.G. Kostianoy, A.N. Kosarev, eds., 2008. *The Black Sea Environment. The Handbook of Environmental Chemistry*. Berlin, Heidelberg: Springer, Vol. 5Q, pp. 277–307. https://doi.org/10.1007/698_5_088

Submitted 25.09.2024; accepted after review 08.11.2024; revised 24.06.2025; published 30.09.2025

About the authors:

Yuri V. Artamonov, Leading Research Associate, Marine Hydrophysical Institute of RAS (2 Kapitanskaya St., Sevastopol, 299011, Russian Federation), DSc (Geogr.), ResearcherID: AAC-6651-2020, ORCID ID: 0000-0003-2669-7304, artam-ant@yandex.ru

Elena A. Skripaleva, Senior Research Associate, Marine Hydrophysical Institute of RAS (2 Kapitanskaya St., Sevastopol, 299011, Russian Federation), PhD (Geogr.), **ResearcherID: AAC-6648-2020, ORCID ID: 0000-0003-1012-515X**, *sea-ant@yandex.ru*

Aleksandr A. Latushkin, Senior Research Associate, Marine Hydrophysical Institute of RAS (2 Kapitanskaya St., Sevastopol, 299011, Russian Federation), PhD (Geogr.), **Researcher ID: U-8871-2019, ORCID ID: 0000-0002-3412-7339**, sevsalat@gmail.com

Aleksandr V. Fedirko, Junior Research Associate, Marine Hydrophysical Institute of RAS (2 Kapitanskaya St., Sevastopol, 299011, Russian Federation), **ResearcherID: AAC-6629-2020, ORCID ID: 0000-0002-8399-3743**, *vault102@gmail.com*

Contribution of the authors:

Yuri V. Artamonov – general scientific supervision of the research, statement of study aims and objectives, development of methods, qualitative analysis of the results and interpretation thereof, discussion of the study results, drawing conclusions

Elena A. Skripaleva – review of literature on the study topic, qualitative analysis of the results and interpretation thereof, processing and description of the study results, discussion of the study results, drawing conclusions, article text preparation and refinement

Aleksandr A. Latushkin – preparation and maintenance of hydro-optical equipment, obtaining *in situ* data, participation in discussion of the article materials

Aleksandr V. Fedirko – development and debugging of software for data processing, computer implementation of algorithms, chart and diagram construction, participation in discussion of the article materials

All the authors have read and approved the final manuscript.